PRODUCTION OF TURBULENT KINETIC ENERGY
From airborne measurements during VTMX 2000

Ronald Dobosy
NOAA Atmospheric Turbulence and Diffusion Division
Oak Ridge TN
2002 October 24

Introduction

Budgets of turbulent kinetic energy (TKE) have stringent sample-size requirements not generally met with airborne measurements. The flights over the Salt Lake Valley during VTMX2000, however, repeated the same track multiple times, allowing some hope of a sufficient sample size. This report describes a preliminary computation of the dominant terms. The results suggest an interesting and plausible pattern in the horizontal structure of TKE generation. Further development of this airborne capability will, we hope provide a useful tool for examining TKE in locations inaccessible to other means of measurement.

Airborne *in-situ* measurements have several unique properties complementary to fixed *in-situ* sensors and to remote sensors. Though fixed sensors can be deployed over extended periods, an airplane provides spatial information unavailable to them. Though remote sensors cover far more space in a given time, airborne instruments directly measure far more of the standard parameters. The airborne measurements thus complement fixed sites' temporal coverage and remote sensors' limited parameter space.

Budget of Turbulent Kinetic Energy

$$\frac{\partial e}{\partial t} = -U_i \frac{\partial e}{\partial x_j} - \overline{u_i' u_j'} \frac{\partial U_i}{\partial x_j} + \frac{g}{\Theta_0} \overline{\theta' u_i'} \delta_{i3} - \frac{\partial}{\partial x_j}\left(\overline{u_j' p'} \frac{1}{\rho_0} \right) - \frac{\partial}{\partial x_j}\left(\overline{u_j' e} \right) - \varepsilon$$

A B C D E F G

The equation above describes the generation, dissipation, transport, and storage of TKE (*e*). Its primary terms are expected to be mechanical and buoyant generation (C and D), and dissipation (G). Storage (A) and (horizontal) mean advection (B) will also be considered.

Budget volume

The budget applies in the two-dimensional neighborhood, radius 3 km, of a point nominally at airplane's altitude over ATDD's towers (-112.0107° longitude, 40.5861° latitude, 1700 m MSL or about 300 m AGL). The neighborhood is assumed to be sufficiently small that departures from horizontal homogeneity are small compared to the mean over the (2D) region. Assume turbulence has sufficiently small scale to justify using 3 km averages (60 s of flight time). This is equivalent to a 600-s average from a stationary sensor, given the wind speed of about 5 ms^{-1}. Velocity profiles taken in ascent from Salt Lake City's Municipal Airport Number Two (SLC#2) sample the vertical gradient of horizontal wind for term C.

Flight Pattern

The airplane followed two racetracks oriented north south, one on the west side and one on the east side of the Salt Lake Valley. This work concerns the racetrack to the west. The parts providing relevant data are shown in Fig. 1. All passes are nominally at the same altitude, about 300 m above ground. Red circles demark the ends of the 3-km segments over which fluxes were calculated. The westernmost path of this west-valley racetrack was always flown northbound, hence designated "WVN." The track passing over SLC2, flown southbound, was designated "WVS." The Oquirrh Mountains are 10 km to the west of the pattern. Nominal flight time was 0300 MST to 0700 MST, ending at local dawn.

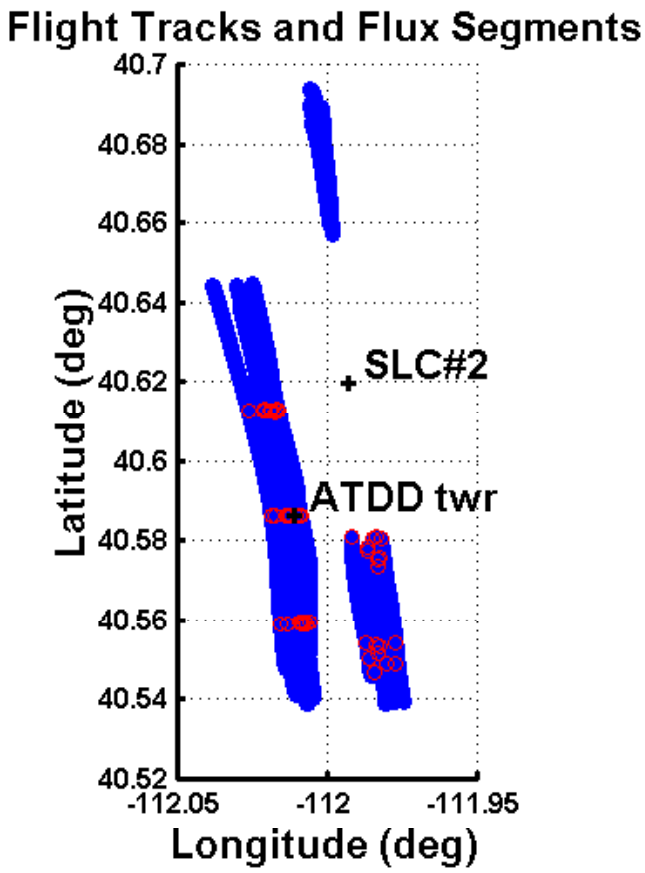

Figure 1

Comparison with TKE from tower

The tower in this preliminary exercise serves primarily for assessing the validity of the airborne measurements of TKE. Tower-derived values are from half-hour averages using detrended quantities. Airborne measurements correspond more to ten-minute averages. Nevertheless, the match in Fig. 2 is good for the second half of the flight. Shallow slope flow or similar may account for stronger TKE at the tower in the first half.

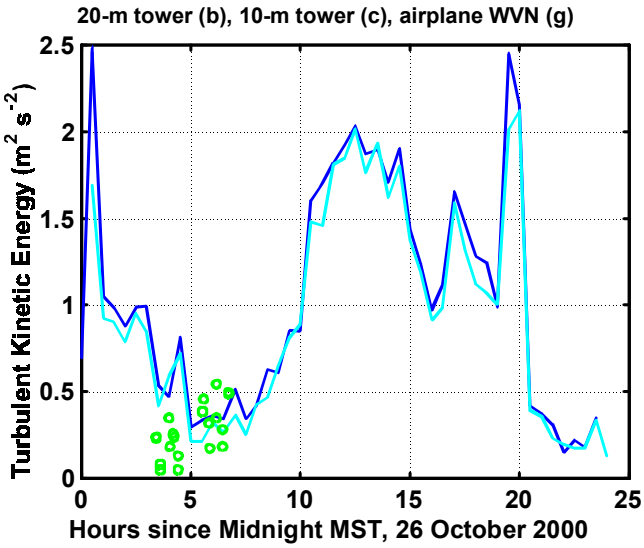

Figure 2: Airplane TKE shown by green circles. Lines show tower data.

Budget Terms: mechanical production

Mechanical production of TKE in the atmospheric boundary layer is by interaction between the vertical gradient of the horizontal mean wind and the vertical flux of horizontal momentum (term C). Three of the ten profiles taken at SLC2 are shown in Figs. 3 and 4. "Down" refers to descent to SLC2, while "up" refers to climbing out from the low pass over the runway. Since "up" profiles were more consistent among each other and were located closer to the

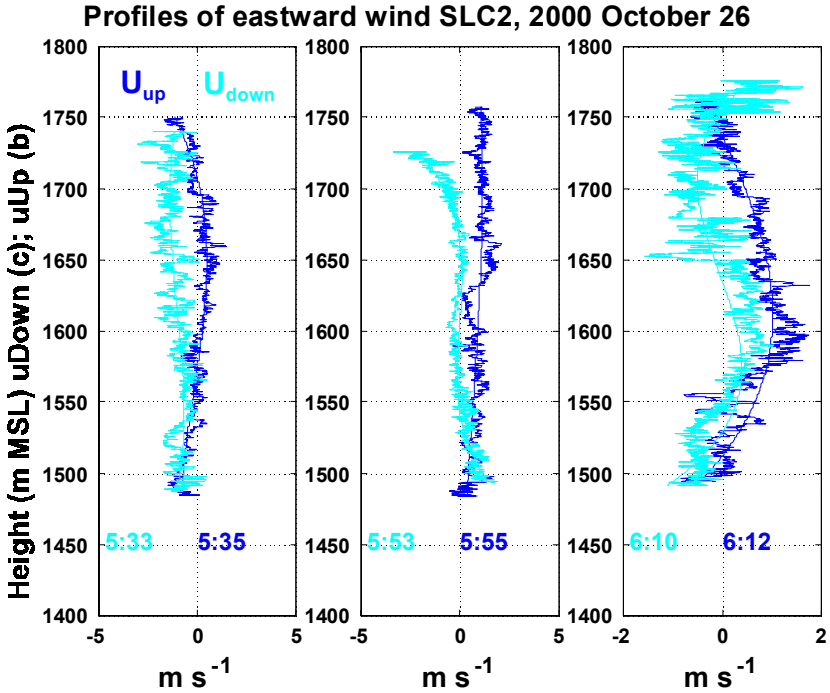

Figure 3: Three of ten profiles. "Down" refers to measurements taken during descent to a low pass over the runway. "Up" refers to the climb out.

sites of the other measurements, only "up" profiles were used to compute the mean velocity gradient. A cubic polynomial was fit to the winds, the slope of which was evaluated at 1700 m MSL, about 300-m above the airport. These computed slopes were plotted on the temporal scatter diagram of Fig. 5. A quadratic polynomial is fit to the points to show their general trend

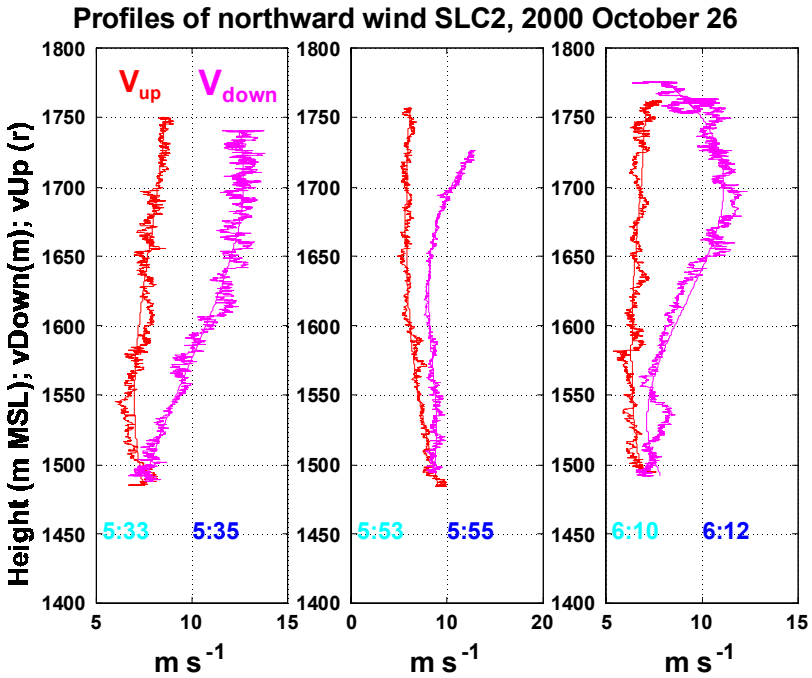

Figure 4: Same as Fig. 3 except northward component.

Vertical flux of horizontal momentum is computed as 3-km averages of cross products between the vertical velocity component (W) and each of the horizontal velocity components (U, V). All quantities are detrended over the 3-km interval before multiplying and averaging. A temporal scatter plot of these results appears also in Fig. 5, again fit with a quadratic polynomial as a visual aid.

The mechanical production was determined by multiplying each computed value of velocity gradient by the three momentum fluxes closest to it in time. The resulting temporal scatter plot is Fig. 6. It has fewer than 30 points because not all flux values corresponded closely in time to a velocity gradient. The pattern shows almost zero mechanical generation in the first half of the flight, with increased generation, and increased scatter, in the second half. A cubic polynomial was selected to fit this pattern, its values serving as estimators for the mechanical production over time. Additional averaging is implied in the polynomial fit, increasing the effective sample size, though not the physical averaging scale of 3 km.

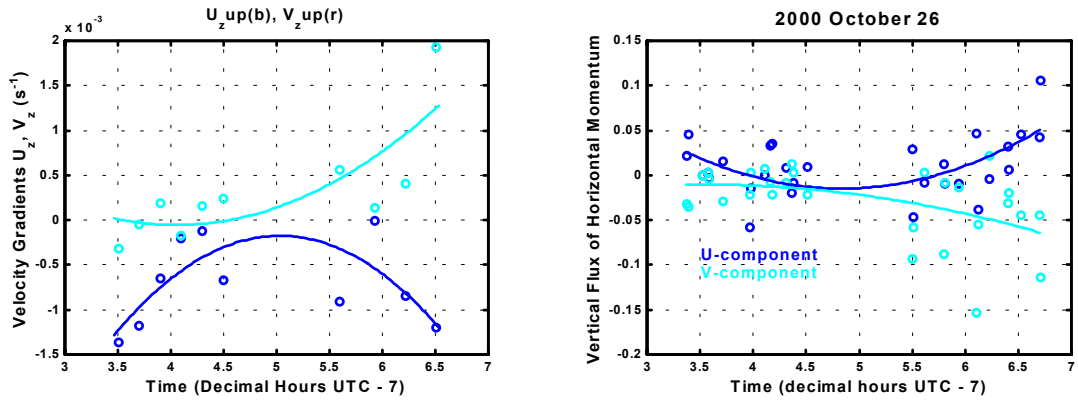

Figure 5: Left: temporal scatter plot of vertical gradients of horizontal velocity. Right: Temporal scatter plot of vertical flux of horizontal momentum. Blue is U, cyan V.

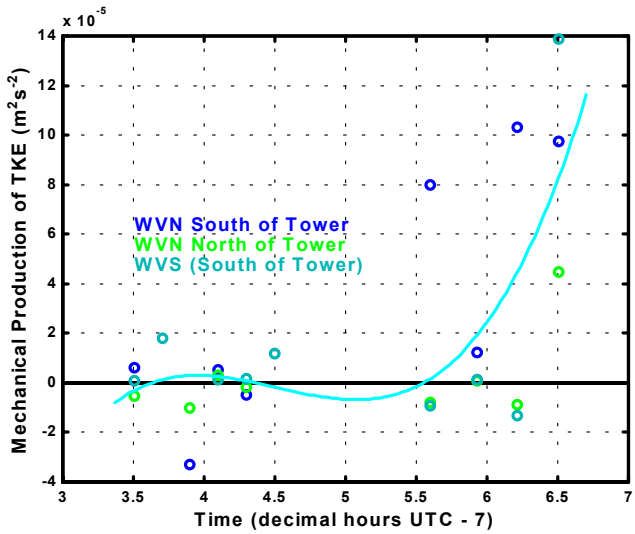

Figure 6: Temporal scatter plot of mechanical generation of TKE. Cubic polynomial fit provides further averaging.

Budget Terms: buoyant production

The buoyant production is far simpler to compute. The covariance of potential temperature with vertical velocity over 3 km is multiplied by the acceleration of gravity (9.8 ms^{-2}) and divided by the mean temperature over the same 3-km interval. A quadratic fit to the temporal scatter plot (Fig. 7) provides the estimator for this term. Note that the heat flux in Fig. 7 must be divided by the air's density and specific heat at constant pressure to obtain the covariance used to compute buoyant production.

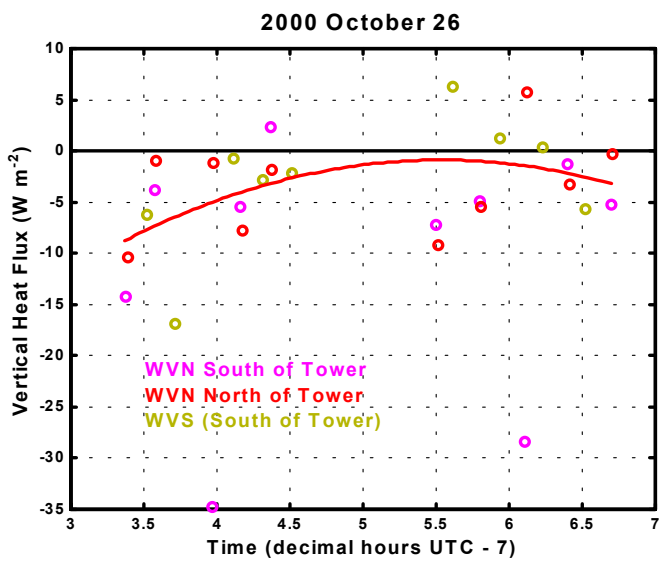

Figure 7: Vertical heat flux for buoyant production. Note small values. Quadratic polynomial fit provides averaging as in Fig. 6

Budget Terms: storage and horizontal advection

Storage depends on the temporal variation of TKE, while advection depends on its variation along the mean wind. Temporal scatter plots of TKE and mean wind appear in Fig 8. Clearly WVS has the lowest TKE, indicating a zonal gradient. However the zonal wind (U) was minimal. Mean vertical motion was assumed zero.

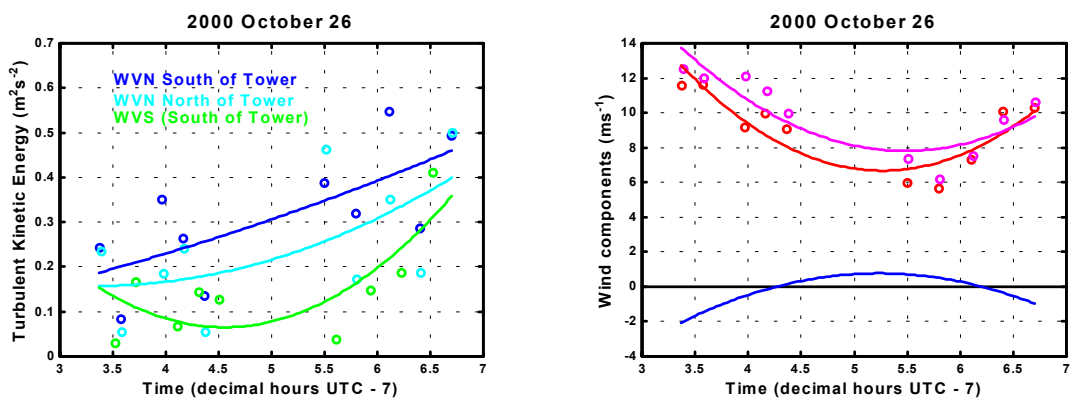

Figure 8: Left: temporal scatter plot of TKE. Right: mean advecting wind components. Northward (V) are red (WVN south of tower) and magenta (WVN north of tower). Blue is eastward (U), not used in the computation. Computations used the quadratic curves.

Hence only the change of TKE from WVN (south) to WVN (north) was used to estimate advection. The advection was computed as a product where the average northward wind (V) over the two WVN segments multiplies the divided difference (over 3 km) in TKE between the two segments. Both the V and the TKE were represented in these calculations by the quadratic fits to their temporal scatter plots (Fig. 8). The time change is estimated by differentiating the average of the two quadratic polynomials fit to the

TKE for WVN (south) and WVN (north). The WVS was not used here because it was measured farther from the tower.

Conclusion

The many simplifications made in producing this preliminary calculation can and need to be tested. Among other things, no attempt has been made to account for gravity waves' influence on this picture. Fig. 9 shows all terms together. Dissipation has not yet been calculated. Encouragingly, the residue is positive through most(!) of the period.

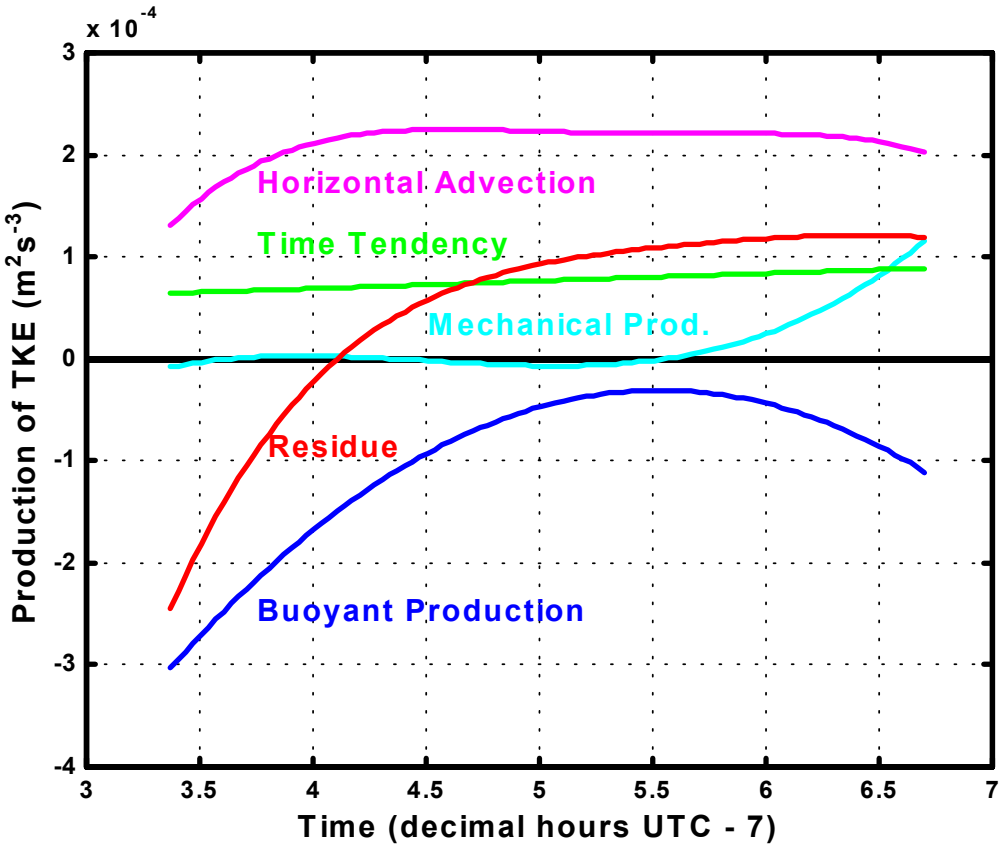

Figure 9: Summary of computed TKE budget terms.

Curiously, the mechanical production is very small, dominated by the buoyant destruction even with such small heat fluxes. If these calculations are valid, they describe turbulence generated to the south and west of the budget region, perhaps by crossing the Traverse Ridge. Apparently the TKE is stronger to the west, closer to the Oquirrh Range. It is being carried northward by the mean flow, decaying as it comes due to viscous dissipation and buoyant destruction. Yet over time, the TKE is strengthening, perhaps due to increasingly strong generation upstream. The mixing upstream may have homogenized the velocity field sufficiently to minimize the mechanical generation at the flight level early in the period. The mechanical generation becomes important toward dawn. This speculative scenario is sufficiently plausible to encourage further examination.